Appl Microbiol Biotechnol (2016) 100:1901–1914
DOI 10.1007/s00253-015-7154-4

APPLIED MICROBIAL AND CELL PHYSIOLOGY

Calcium fluoride nanoparticles induced suppression of *Streptococcus mutans* biofilm: an in vitro and in vivo approach

Shatavari Kulshrestha[1] · **Shakir Khan**[1] · **Sadaf Hasan**[1] · **M. Ehtisham Khan**[2] · **Lama Misba**[1] · **Asad U. Khan**[1]

Received: 12 June 2015 / Revised: 24 October 2015 / Accepted: 6 November 2015 / Published online: 27 November 2015

Abstract Biofilm formation on the tooth surface is the root cause of dental caries and periodontal diseases. *Streptococcus mutans* is known to produce biofilm which is one of the primary causes of dental caries. Acid production and acid tolerance along with exopolysaccharide (EPS) formation are major virulence factors of *S. mutans* biofilm. In the current study, calcium fluoride nanoparticles (CaF_2-NPs) were evaluated for their effect on the biofilm forming ability of *S. mutans* in vivo and in vitro. The in vitro studies revealed 89 % and 90 % reduction in biofilm formation and EPS production, respectively. Moreover, acid production and acid tolerance abilities of *S. mutans* were also reduced considerably in the presence of CaF_2-NPs. Confocal laser scanning microscopy and transmission electron microscopy images were in accordance with the other results indicating inhibition of biofilm without affecting bacterial viability. The qRT-PCR gene expression analysis showed significant downregulation of various virulence genes (*vicR*, *gtfC*, *ftf*, *spaP*, *comDE*) associated with biofilm formation. Furthermore, CaF_2-NPs were found to substantially decrease the caries in treated rat groups as compared to the untreated groups in in vivo studies. Scanning electron micrographs of rat's teeth further validated our results. These findings suggest that the CaF_2-NPs may be used as a potential antibiofilm applicant against *S. mutans* and may be applied as a topical agent to reduce dental caries.

Keywords Calcium fluoride nanoparticles · *Streptococcus mutans* · Biofilm · Dental caries · qRT-PCR · Virulence factors

Introduction

Dental caries are characterized by dissolution of the tooth enamel and are a cause of public health concern (Nakano et al. 2007; Falsetta et al. 2014). A major factor influencing dental decay is an assault of the tooth surface by oral microbial biofilms (Selwitz et al. 2007; Nance et al. 2013). *Streptococcus mutans* is considered to be one of the main etiological agents of dental caries and is a best known biofilm-forming oral bacterium (Loesche 1986; Hasan et al. 2015). Acid production by fermentation of dietary carbohydrate (acidogenesis), formation of exopolysaccharide, and biofilm formation along with its ability to survive in an acidic environment (aciduracity) are some of the prominent characteristics which help *S. mutans* in its cariogenic process (Koo et al. 2003; Krol et al. 2014). Eradication of dental biofilm is very difficult and only mechanical cleaning like brushing or flossing the teeth is not sufficient. Thus, to improve oral health, it is important to formulate approaches that can inhibit or delay biofilm formation.

Fluorides and its various preparations are of great importance in dentistry (Marquis et al. 2003). In its ionic form, fluoride prevents demineralization and helps in remineralization of the tooth enamel (Featherstone 1999). Fluorides also exert their effect on the biological activity of caries-causing bacteria. They reduce the ability of plaque-forming bacteria to produce acid and can impair glycolysis by inhibition of enolase activity (Hamilton 1977).

Electronic supplementary material The online version of this article (doi:10.1007/s00253-015-7154-4) contains supplementary material, which is available to authorized users.

✉ Asad U. Khan
asad.k@rediffmail.com

[1] Interdisciplinary Biotechnology Unit, Aligarh Muslim University, Aligarh 202002, India

[2] Center of Excellence in Material Sciences (Nanomaterials), Aligarh Muslim University, Aligarh 202002, India

Furthermore, they work on membrane-associated proton pump (H^+-ATPase) by inhibiting it and in turn reducing the cellular level of ATP (Sutton et al. 1987; Eshed et al. 2013).

It is believed that topical application of fluoride on teeth leads to the formation of a calcium fluoride-like material which acts as a reservoir of fluoride ions, and during caries challenge, it releases fluoride at low pH in plaque and protects the tooth's surface from caries (Rosin-Grget and Lincir 2001; Rølla and Saxegaard 1990). Nevertheless, the limited concentration of calcium ion in the mouth results in the formation of only a limited amount of calcium fluoride-like deposits after topical application of conventional fluoride formulations (Saxegaard and Rølla 1989).

Nanoscale-based approaches are being widely used and have been proven to be more effective in the elimination of biofilms and in the inhibition of dental caries (Eshed et al. 2013; Kulshrestha et al. 2014; Hernández-Sierra et al. 2008). Their high surface to volume ratio provides them with unique properties which can be exploited for the development of new therapies and drugs (Raghupathi et al. 2011). Sun and Chow have demonstrated that a calcium fluoride nanoparticle (CaF_2-NP) rinse can increase the level of fluoride ions in the oral fluid, and in another study, the strength and the fluoride release capacity of a dental composite having CaF_2-NPs have been shown (Sun and Chow 2008; Xu et al. 2008). However, there are no studies focusing on the direct effect of CaF_2-NPs on caries causing virulence factors like exopolysaccharide production, biofilm formation, aciduracity and acidogenesis of *S. mutans* as well as its effect on demineralization of the dental enamel.

The main objective of this study was to formulate CaF_2-NPs and to evaluate its effect on some of the major virulence factors of *S. mutans*. Furthermore, we had investigated the effect of CaF_2-NPs on caries development in an in vivo model to evaluate its use as a topical agent for the prevention of dental caries.

Materials and methods

Microorganisms

UA159 strain of *S. mutans*, purchased from IMTECH, Chandigarh, India (MTCC SM497), was used in this study. All the strains were grown in a brain heart infusion broth (BHI) (HiMedia Laboratories, Mumbai, India) at 37 °C. The cultures were stored at −80 °C in BHI containing 25 % glycerol.

Nanoparticle formation

CaF_2-NPs were synthesized by a simple coprecipitation method as described earlier with slight modification (Pandurangappa and Lakshminarasappa 2011a, b). In a typical procedure, calcium chloride ($CaCl_2$) and ammonium fluoride (NH_4F) were dissolved in 100 ml distilled water in a molar ratio of 1:2, and the mixture was continuously stirred for 2 h using a magnetic stirrer. The calcium fluoride nanoparticle formation was indicated by the gradual color change from transparent to opaque white suspension. After that, few drops of ammonia were added into the mixture for precipitation. The stirred solution was centrifuged for 15 min at 8000 rpm and a white residue was obtained. The residue was washed thoroughly with ethanol and water. The obtained product was kept in a ceramic petri dish and dried slowly in a vacuum oven overnight at 60 °C and sintered at 300 °C for 3 h.

Characterization of calcium fluoride nanoparticles

The synthesis of CaF_2-NPs in the solution was monitored by measuring absorbance using a UV-visible spectrophotometer (PerkinElmer Life and Analytical Sciences, CT, USA) in the wavelength range of 200 to 800 nm. Transmission electron microscopy (TEM) analysis was performed using a JEM-2100F TEM (Jeol, Tokyo, Japan) operating at 120 kV, and nanoparticle size was calculated by examining a TEM image by the ImageJ software (ImageJ 1.46r; Java 1.6.0_20). Scanning electron microscopy (SEM) has also been employed to study the surface topography of CaF_2-NPs. X-ray diffraction (XRD) patterns of the powdered sample were recorded on a MiniFlex™ II bench top XRD system (Rigaku Corporation, Tokyo, Japan) operating at 40 kV. For the Fourier transform infrared spectroscopic (FTIR) measurements, CaF_2-NPs were mixed with spectroscopic grade potassium bromide (KBr) in the ratio of 1:100, and the spectra were recorded in the range 400–4000 wavenumber (cm^{-1}) on a Perkin Elmer FTIR Spectrum BX (PerkinElmer Life and Analytical Sciences) in the diffuse reflectance mode at a resolution of 4 cm^{-1} in KBr pellets.

Determination of bacteriostatic (MIC) and bactericidal (MBC) concentrations

The minimum inhibitory concentration (MIC) of CaF_2-NPs against *S. mutans* was determined using a double dilution method as described earlier (Kulshrestha et al. 2014). The minimum bactericidal concentration (MBC), on the other hand, was determined by subculturing the test dilutions on BHI agar plates and incubating for 24 h. The concentration at which there was no growth on agar plates was taken as MBC. The determinations were performed in triplicate and the means of three independent experiments were calculated.

Biofilm formation assay

Biofilm formation was estimated by crystal violet assay. An overnight culture of *S. mutans* was diluted to 10^5–10^6 colony

forming units (cfu)/ml and 50 μl of diluted culture was inoculated into 100 μl of fresh media (BHI+5 % sucrose) containing various sub-MIC concentrations of nanoparticles. A medium devoid of nanoparticle was used as a control. The microtiter plates were incubated at 37 °C for 24 h. After incubation, the medium was decanted and the remaining planktonic cells were removed by gently rinsing with sterile water. The adhered biofilms were stained with 200 μl of 0.1 % crystal violet dye for 15 min at room temperature. After gentle washing with distilled water, the bound dye was removed from the cells with 100 μl of 98 % ethanol. For the full release of the dye, the plates were kept on a shaker for 5 min. Biofilm formation was quantified by measuring the optical density $(OD)_{630}$ using a Bio-Rad iMark^{TM} Microplate reader, India.

Estimation of exopolysaccharide production

The Congo red (CR) binding assay was used to evaluate exopolysaccharide (EPS) production. Biofilms were grown in the presence of various concentrations of CaF_2-NPs in a microtiter plate. Fifty microliters of Congo red dye (0.5 mM) was added to each well. The medium (100 μl) along with 50 μl of CR was used as blank. The microtiter plate was then incubated at 37 °C for 60 min. After incubation, the medium of each well was transferred in a separate microcentrifuge tube and centrifuged at 10,000*g* for 5 min. Two hundred microliters of supernatant was separated from each tube and absorbance was measured at 490 nm. The untreated sample was taken as control. This experiment was conducted in triplicate. The amount of EPS produced was estimated using the following formula (López-Moreno et al. 2014):

$$\text{OD of blank CR} - \text{OD of the supernatant} = \text{OD of bound CR(EPS produced)}$$

Effect on growth curve

Overnight culture of *S. mutans* was diluted in fresh BHI media to get (OD_{600}) 0.01 followed by the addition of 4, 2, and 1 mg ml^{-1} CaF_2-NPs. Both control and treated cultures were incubated at 37 °C for 24 h. Growth was monitored every hour by taking the absorbance at 600 nm. The experiment was performed in triplicate and the untreated samples were used as controls.

Effect on adherence of *S. mutans*

The glass surface adherence assay was performed to evaluate the effect of CaF_2-NPs on adherence of *S. mutans* (Hamada and Slade 1980). The bacteria (~5×10^5 CFU/ml) were grown for 6 h at 37 °C at an angle of 30° in a glass tube containing BHI with 5 % sucrose and various concentrations of CaF_2-NPs (4, 2, and 1 mg ml^{-1}). The solvent controls included BHI (with 5 % sucrose) and an equivalent amount of nanoparticles. After incubation, planktonic cells were decanted, and the attached cells were removed by 0.5 M of sodium hydroxide. Planktonic and adhered cells were quantified using a UV spectrometer by taking OD at 600 nm. Percent adherence was calculated using the following formula:

$$\% \text{ Adherence} = \left(\text{OD}_{600}\text{of adhered cells} \Big/ \text{OD}_{600}\text{ of total cells}\right) \times 100$$

Effect on preformed biofilm

Approximately 10^7 cfu/ml of *S. mutans* cells was added to each well of sterile 96-well microtiter plates. The plates were then incubated at 37 °C for 24 h to form the biofilm. Then, the supernatant containing planktonic cells was removed and washed three times using 100 μl 0.9 % (*w*/*v*) NaCl. The preformed biofilms were incubated at 37 °C in the media (BHI+5 % sucrose) containing different concentrations of CaF_2-NPs (4, 2, and 1 mg ml^{-1}) for 24 h. Biofilm mass was evaluated by crystal violet assay.

Inhibition of water-insoluble and water-soluble glucan synthesis

The crude glucosyltransferase (GTF) was prepared from the cell-free supernatant of *S. mutans* culture and assayed to evaluate the effect of nanoparticles on glucan synthesis. The enzyme was precipitated from the supernatant by a previously reported method (Hasan et al. 2012). A reaction mixture consisting of 0.25 ml of crude enzyme, varying concentrations of nanoparticles in 20 mM phosphate buffer (pH 6.8), and 0.25 ml of sodium acetate buffer (pH 5.7, having 0.4 M sucrose) was incubated at 37 °C for 2 h. The mixture was then centrifuged at 10,000*g* for 5 min to separate water-soluble and water-insoluble glucans. Total amounts of water-soluble and insoluble glucans were measured by the phenol-sulfuric acid method (Dubois et al. 1956). Three replicates were made for each concentration of the test compounds.

Glycolytic pH drop assay and acid production

Glycolytic pH drop of *S. mutans* was estimated as described elsewhere (Phan et al. 2004). Cells were harvested from the suspension culture by centrifugation and washed with a salt solution (50 mM KCl+1 mM $MgCl_2$). The cells were then resuspended in a fresh salt solution containing different concentrations (4, 2, and 1 mg ml^{-1}) of nanoparticles. The pH was

adjusted between 7.2 and 7.4 with 0.2 M KOH solution followed by the addition of glucose (1 % *w/v*). The decrease in pH was assessed every 10 min over a period of 60 min using a pH meter. The initial rate of the pH drop, which can give the best measure of the acid production capacity of the cells, was calculated using the pH values in the linear portion (0–10 min).

RNA extraction, reverse transcription and quantitative real-time PCR

To analyze the effect of CaF_2-NP treatment on the expression of virulence genes of *S. mutans*, quantitative real-time PCR (qRT-PCR) was performed. The organism was cultured in BHI media supplemented with CaF_2-NPs (4 mg ml^{-1}). Bacterial culture (OD_{600}=1) was diluted (1:10) and inoculated into fresh BHI media, followed by overnight growth at 37 °C. RNA was isolated using TRIzol reagent (Invitrogen, Life Technologies). Purified RNA was dissolved in diethylpyrocarbonate-treated water and was stored at −80 °C until required for complementary DNA (cDNA) preparation. cDNA was prepared using a High Capacity cDNA Reverse Transcription Kit (Applied Biosystems, Foster City, USA). The reverse transcription reaction mixture (20 μl) contained 2 μl 10× reverse transcriptase (RT) buffer, 0.8 μl 25× dNTP Mix (100 m M), 2 μl 10× RT random primers, 1 μl MultiScribe™ reverse transcriptase, 1 μg of RNA, and nuclease-free H_2O to make up the volume. It was incubated at 25 °C for 10 min, followed by incubation at 37 °C for 120 min. Finally, the reaction was terminated by incubating the mixture at 85 °C for 5 min according to the manufacturer's instructions. cDNA samples were stored at −20 °C for further use.

The *vicR*, *gtfC*, *spaP*, *comDE*, and *ftf* primers (Table 1) were designed using the algorithms provided by Primer Express (Applied Biosystems) for uniformity in size (≤95 bp) and melting temperature. PCR conditions included an initial denaturation at 95 °C for 10 min, followed by 40 cycles of amplification with each cycle having denaturation at 95 °C for 15 s and annealing and extension at 60 °C for 1 min. The expression levels of all the tested genes were normalized using the 16S ribosomal RNA (rRNA) gene of *S. mutans* as an internal standard (Livak and Schmittgen 2001).

Confocal microscopy

Confocal microscopy was performed in order to view the changes in biofilm formation. Covered glass bottom dishes (Genetix Biotech Asia) were used to grow *S. mutans* biofilm in the presence and absence of CaF_2-NP (4, 2, and 1 mg ml^{-1}) at 37 °C. The cells of the biofilm were stained with SYTO-9 (5 μM; excitation wavelength of 488 nm and emission wavelength of 498 nm) and propidium iodide (PI) (0.75 μM; excitation wavelength of 536 nm and emission wavelength of 617 nm). The stained bacterial biofilm was observed with a FluoView FV1000 (Olympus, Tokyo, Japan) confocal laser scanning microscope equipped with argon and He-Ne laser.

Transmission electron microscopy

Transmission electron microscopy was used to investigate the intracellular changes in *S. mutans* (Khan et al. 2012). Control and nanoparticle-treated culture material were suspended using a centrifuge and washed with PBS (pH 7.4). Secondary fixation was done with 2.5 % glutaraldehyde (HiMedia) and 1 % osmium tetroxide (OsO_4) 2–3 h at 4 °C. Samples were dehydrated by ethanol and embedded in araldite CY212 (Taab, Aldermaston, UK) resin for making the cell-pellet blocks. Ultrathin sections of cells were stained with uranyl acetate and lead citrate and observed under the TEM (Jeol, Tokyo, Japan) microscope at 120 kV.

Toxicity assay on HEK-293 cell line

Cytotoxicity assay was performed on human embryonic kidney cell line (HEK-293) obtained from the National Centre for Cell Science (NCCS), Pune. The cell line was cultured in Dulbecco's modified Eagle's medium (DMEM) supplemented with 10 % heat-inactivated fetal calf serum and IX Penstrep antibiotic solution, incubated at 37 °C and 5 % CO_2. The 3-(4, 5-dimethylthiazol-2-yl)-2,5-diphenyltetrazolium bromide (MTT) assay was used to measure the viability of HEK-293 as described earlier (Denizot and Lang 1986). Various concentrations of CaF_2-NPs (4, 2, and 1 mg ml^{-1}) were incubated with adherent HEK-293 for 24 h. After incubation, the supernatants were removed and 90 μl of fresh medium containing 10 μl of MTT (1 mg ml^{-1}) solution was dispensed in each well. The plates were further incubated for 4 h. The formazan crystals formed by the cellular reduction of MTT were dissolved in 150 μl of DMSO, and the plates were read on an ELISA reader using a 570-nm filter. Wells containing cells without treatment were used as controls. All measurements were done in triplicate.

In vivo toxicity studies

Acute oral toxicity of the nanoparticles was evaluated in accordance with the Organization for Economic and Cooperation Development (OECD) guidelines (1998) for testing chemicals. A limit test (2000 mg kg^{-1} body weight of the animal) was carried out using five male Wistar rats in each group (treated and control) ranging from 150 to 200 g in weight. These animals were housed in standard hard bottom, polypropylene cages. They were fed with standard pelletized diet and sterile tap water ad libitum. All animals were observed for changes in their weight, behavior, and mortality till

Table 1 Nucleotide sequences of primers used in this study database (NCBI)

Gene[a]	Description	Primer sequence (5′–3′)	
		Forward	Reverse
16S rRNA	Normalizing internal standard	CCTACGGGAGGCAGCAGTAG	CAACAGAGCTTTACGATCCGAAA
vicR	Two-component regulatory system	TGACACGATTACAGCCTTTGATG	CGTCTAGTTCTGGTAACATTAA GTCCAATA
gtfC	Glucosyl transferase C (GTF C); glucan production	GGTTTAACGTCAAAATTAGCTG TATTAGC	CTCAACCAACCGCCACTGTT
ftf	Fructosyl transferase (FTF); fructan production	AAATATGAAGGCGGCTACAACG	CTTCACCAGTCTTAGCATCCTGAA
spaP	Cell surface antigen, SpaP (or Ag I/II)	GACTTTGGTAATGGTTATGCATCAA	TTTGTATCAGCCGGATCAAGTG
comDE	Competence-stimulating peptide	ACAATTCCTTGAGTTCCATCCAAG	TGGTCTGCTGCCTGTTGC

[a] Based on *S. mutans* genome

the 14th day post-administration of dose. Efforts were made to minimize animal suffering and the number of animals for experimentation purpose.

Caries induction in rats

To determine the effects of CaF_2-NPs on oral establishment and cariogenic potential of *S. mutans*, a total of 20 rats were purchased. These animals were divided into two groups: a control and a test group (n=10 per group). All the animals were fed with erythromycin water (100 μg ml^{-1}) and a regular diet for 3 days in order to reduce the microbial load. To confirm the absence of *S. mutans* colonization in the oral cavity, oral swabs were plated on mitis salivarius-bacitracin (MSB) agar plates. The animals were offered 5 % sucrose diet ad libitum throughout the experiment in order to enhance the infection by *S. mutans*. On the 4th day, their molar tooth surfaces were inoculated with a streptomycin-resistant strain of *S. mutans*—MT8148R (1.4×10^{10} cfu). The inoculation was repeated once every day for five consecutive days. After that CaF_2-NPs were topically applied twice a day on the teeth of animals by means of a camel hairbrush for 2 weeks. Swab samples were then taken from the surfaces of animal molars on the first day of the first, third, sixth, eighth, and tenth week postinoculation. The samples from the control and treated groups were pooled in 2 ml of 10 mM potassium phosphate buffer, serially diluted, and plated on MSB agar plates containing streptomycin for total cell counts. The plates were incubated at 37 °C for 2 days before enumeration of colonies of *S. mutans*. The percentages of the *S. mutans* cells were calculated to determine its oral colonization in the animals. At the end of the experimental period, all the animals were sacrificed. The jaws were then aseptically dissected and sonicated in 5 ml of 154 mM sterile NaCl in order to dislodge the dental plaque. These samples of plaque were serially diluted and were streaked on mitis salivarius agar plates to estimate the *S. mutans* population. These plates were incubated at 37 °C for 2 days before enumeration of colonies. All of the jaws were defleshed and suspended in 3.7 % formaldehyde until caries scoring. All molars of the animals were examined under a dissecting microscope and carious lesions were scored by a Larson's modification of the Keyes system (Larson 1981). The results obtained were analyzed by Student's t test, with $p<0.05$ considered as statistically significant.

Scanning electron microscopy of animal tooth's surface

The effect of the CaF_2-NPs on the structural integrity of the biofilm and subsequent reduction in caries formation was also observed by SEM. The aseptically removed jaws of the animals (Wistar rats) were stored in normal saline and were directly visualized under SEM. The experiment was performed in triplicate. The samples were analyzed by SEM (Hitachi S-3000N; High Technology Operation, Japan) at several magnifications.

Statistical analysis

The values were calculated as the mean of individual experiments in triplicate and compared with those of the control groups. Differences between two mean values were calculated by Student's t test. A one-way analysis of variance (ANOVA) was performed for comparison of multiple means using the online link: http://www.physics.csbsju.edu/stats/anova.html. Data with p values <0.05 were considered statistically significant. For qRT-PCR, one-way ANOVA was followed by post hoc multiple comparisons (Tukey's test) to compare the multiple means using the R software (ver 3.2.0). Values were considered statistically significant when p value was <0.05.

Results

Characterization of calcium fluoride nanoparticles

TEM analysis of CaF_2-NPs was performed to determine its morphology and size (Fig. 1a). The particles were found to be

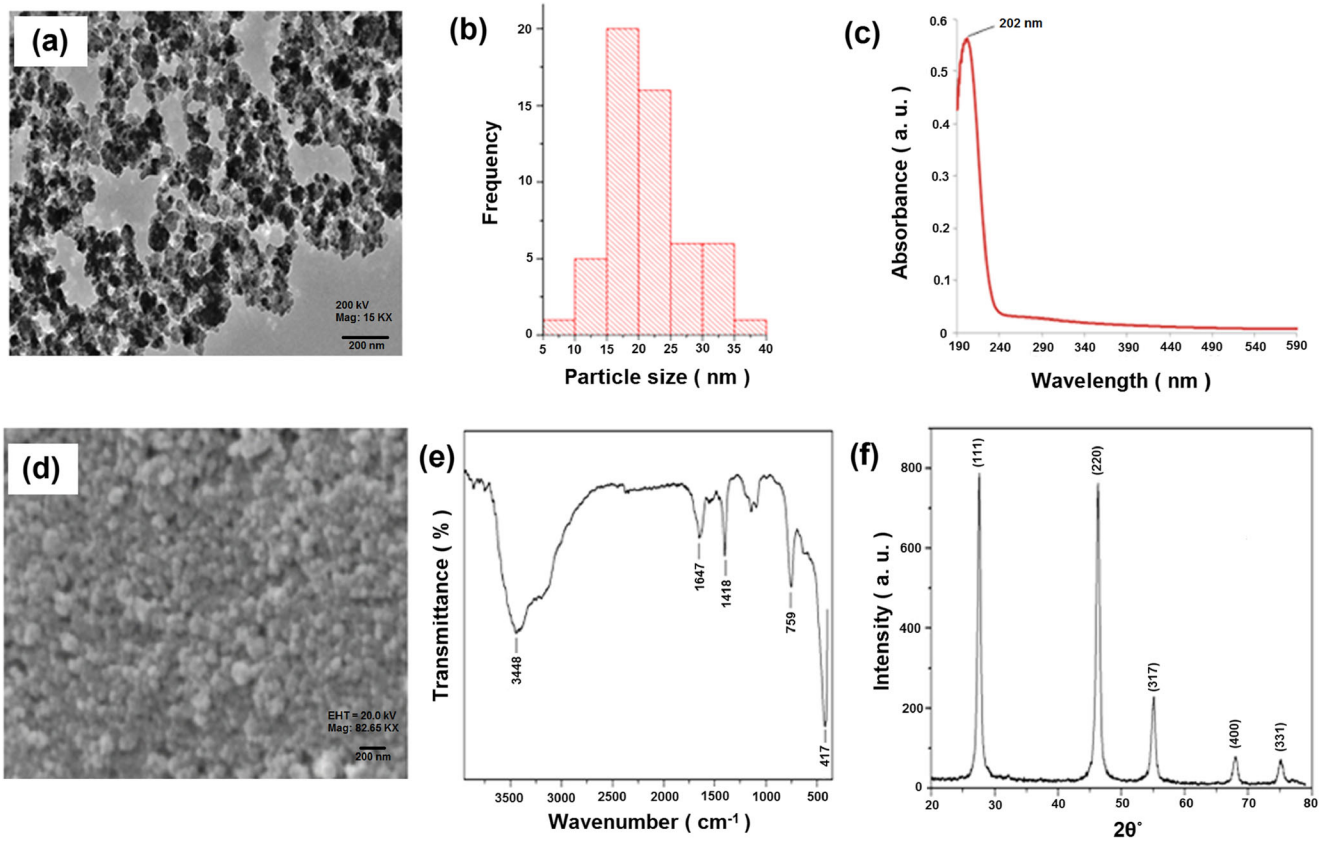

Fig. 1 Characterization of CaF_2-NPs. **a** Transmission electron microscopy image of CaF_2-NPs. **b** Particle size ~15–25 nm. **c** UV-visible absorption spectra CaF_2-NPs. **d** Scanning electron microscopy image of CaF_2-NPs. **e** FTIR spectrum. **f** XRD pattern of CaF_2-NPs

in the nanometer range with an average particle size of 15–25 nm (Fig. 1b). The SEM image (Fig. 1d) of nanoparticles revealed the morphology of the synthesized nanoparticles. The particles were not readily dispersed, but numerous spherical protuberances were observed in the image suggesting that they are formed by aggregation of smaller particles.

UV-visible spectroscopy of the nanoparticle is represented in Fig. 1c. A strong peak was observed in the UV range (~202 nm). CaF_2-NPs show characteristic absorption peaks in the UV range (Pandurangappa and Lakshminarasappa 2011a, b). The origin of these bands is due to the nanosize of the particle. It has been suggested that the large surface to volume ratio of nanoparticles results in the development of voids on the surface and inside the agglomerated nanoparticles. These voids lead to fundamental adsorption in the UV range (Kumar et al. 2007). Furthermore, it is well established that the surface of nanoparticle is comprised of numerous defects like Schottky or Frenkel resulting in the absorption of light by the nanocrystal (Zhang et al. 2008). Thus, the absorption band at 202 nm in the present study confirms the formation of CaF_2-NPs.

The FTIR spectrum of CaF_2-NPs showed a strong band at ~3400, 1678, and 430 cm^{-1} (Fig. 1e). Two peaks at ~3400 and ~1678 cm^{-1} in the FTIR spectrum are due to H-O-H bending of the water molecule. The band at ~430 cm^{-1} arises due to hindered rotation of hydroxyl ion (Khan et al. 2013). Furthermore, Fig. 1f is a typical XRD pattern of CaF_2-NPs. The peaks were indexed using PowderX software and they were well matched with the standard JCPDS No. 87-0971 (Pandurangappa and Lakshminarasappa 2011a, b) which reveals a cubic-phase fluorite-type structure (Fujihara et al. 2002). The broad peaks in the XRD pattern suggest a small crystalline size (Pandurangappa and Lakshminarasappa 2011a, b). The crystalline size was calculated to be ~6.8 nm by using Scherrer's formula. Moreover, from the XRD spectra, it can be estimated that the particles are in a single phase and the pure sample has been synthesized as there are no extra peaks found.

Effect on bacterial viability

The MIC of CaF_2-NPs on *S. mutans* was found to be >64 mg/ml.

Significant reduction in biofilm

Biofilm formation ability of *S. mutans* in the presence of different concentrations (4, 2, 1 mg ml^{-1}) of CaF_2-NPs was evaluated using crystal violet assay (Fig. 1a). There were almost 89, 71, and 62 % reductions in the biofilm-forming ability of

S. mutans as compared to those of the control when treated with 4, 2, and 1 mg ml^{-1} concentrations of nanoparticles, respectively. With the decrease in nanoparticle concentrations, there is a gradual increase in its biofilm formation ability. This suggests a concentration-dependent reduction in biofilm formation.

Effect on EPS production

A considerable decrease in EPS production in *S. mutans* in the presence of CaF_2-NPs was observed and the reduction is in a concentration-dependent manner (Fig. 2b). A 90, 65, and 64 % decrease in EPS production was observed when treated with 4, 2, and 1 mg ml^{-1} of CaF_2-NPs, respectively, as compared to that of the untreated sample. The highest EPS production was seen in the control when no nanoparticles were present. When nanoparticle concentration increased, the EPS production decreased.

Variation in the growth curve of *S. mutans*

Growth curve was used to investigate the effect of CaF_2-NPs on *S. mutans* growth. The results displayed a typical sigmoidal pattern and there was no significant variation between the control and treated samples (Fig. 3). The results clearly indicated that bacterial growth is not hindered at concentrations of nanoparticles used in the study.

Effect on adherence of *S. mutans*

The inhibitory effect of different concentrations of CaF_2-NPs on initial adherence of *S. mutans* is shown in Fig. 4. There were 70, 57, and 44 % inhibition of attachment of *S. mutans* to the glass surface in the presence of 4, 2, and 1 mg ml^{-1} concentrations of CaF_2-NPs, respectively.

Dispersion of preformed biofilm

Different concentrations of CaF_2-NPs were used to evaluate the effect on treatment of preformed biofilm of *S. mutans* (Fig. 4). There were 11, 7, and 5 % reductions of preformed biofilm on treatment with 4, 2, and 1 mg ml^{-1} concentrations of CaF_2-NPs, respectively.

Reduction in glucan production

A significant reduction in both water-insoluble glucan and water-soluble glucan production was observed in *S. mutans* when treated with CaF_2-NPs (Fig. 5). Almost 90 % reduction was observed in the treated sample as compared to the control. Soluble and insoluble glucans both were reduced to the same extent in the present experiment.

Decrease in the rate of acid production and stress tolerance in *S. mutans*

As shown in Fig. 6, the acid tolerance ability of *S. mutans* was inhibited appreciably in the presence of CaF_2-NPs. The onset pH of 7.2 dropped to 4.5 in the control, while in the treated samples (4 mg ml^{-1}), final pH was 5.2. Furthermore, the rate of initial pH drop in 10 min was calculated to be 0.14 to 0.09 min^{-1} in case of the control and treated samples, respectively, demonstrating a pronounced reduction in the acid production ability of *S. mutans*.

Expression profile of virulence gene

qRT-PCR was performed to gain insight into the effect of CaF_2-NP treatment on the expression of virulence genes (*gtfC*, *vicR*, *ftf*, *comDE*, *spaP*) in *S. mutans*. An entire set of genes was downregulated after treatment with nanoparticles (Fig. 7). The expression of *spaP* decreased by 80 % and that of *vicR* and *comDE* genes by >50 %. The decrease in the expression

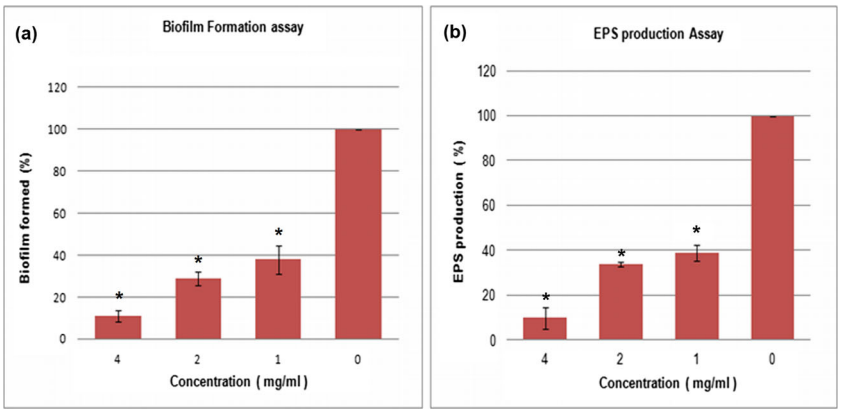

Fig. 2 Inhibitory effect of sub-MIC concentration of CaF_2-NPs. **a** Biofilm formation. **b** EPS production. Data are mean±SD (n=3). Statistical significance as compared with the untreated control (p<0.05) denoted by an *asterisk* (*)

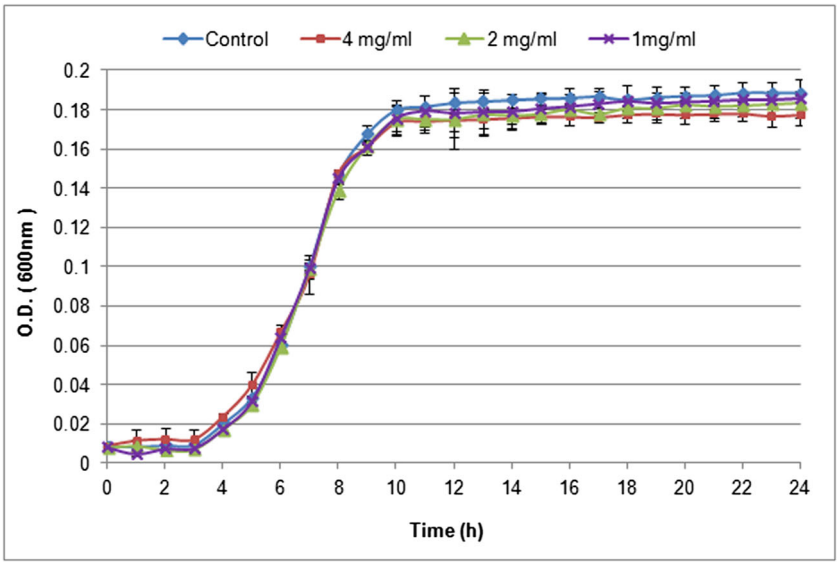

Fig. 3 Growth curves of CaF_2-NP-treated and untreated *S. mutans* (OD values, 1:10 times diluted). The data represent mean ±SD

of *gtfC* gene was 32 % and a suppression of 14 % was observed in the expression of *ftf* gene.

Impairment of biofilm architecture visualized through confocal microscopy

Confocal laser scanning microscopy (CLSM) images of *S. mutans* illustrate an apparent obliteration of biofilm architecture in the presence of CaF_2-NPs without affecting its growth (Fig. 8). The upper panel shows the control sample images, while lower three panels represent images of biofilms when treated with various concentrations of CaF_2-NPs. In the control images (Fig. 8a–d), majority of the cells show green fluorescence with a mat of *S. mutans* cells showing a rich biofilm architecture, while in the treated samples (Fig. 8e–h), cells were highly dispersed and alive, which depicted the inhibition of biofilm formation and not the viability.

Insignificant effect on the cell wall of *S. mutans*

TEM analysis was performed to visualize the effect of nanoparticle on the cell wall of *S. mutans* (Fig. S1 in the Supplementary material). In the control, the cell wall is intact with the healthy intracellular content of bacterium (Fig. S1a); on the contrary, in the image of the treated samples (Fig. S1b), little damage was observed (indicated by red arrows), but the damage was not prominent and majority of the cells were having an intact membrane. The results suggest that there was insignificant damage to the cell walls in the presence of CaF_2-NPs.

Cytotoxicity

The relative cell viability of HEK-293 cell line in the presence of CaF_2-NPs is shown in Fig. S2. Almost 100 % viability was observed in all concentrations (4, 2, and 1 mg ml^{-1}). Thus, the test concentration of CaF_2-NPs is nontoxic to HEK-293 cell line.

Toxicity profile

No mortality was observed after the oral toxicity assay and animals did not exhibit any behavioral or weight changes, thus

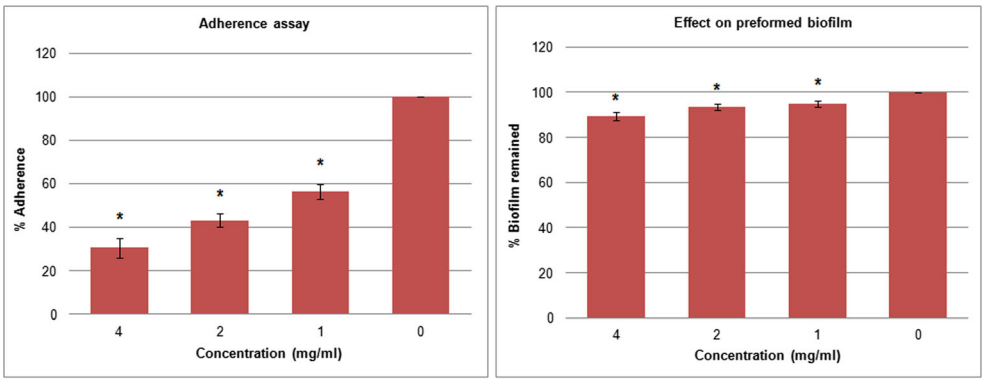

Fig. 4 Inhibitory effect of sub-MIC concentration of CaF_2-NPs on adherence and preformed biofilm of *Streptococcus mutans*. Data are mean±SD (n=3). Statistical significance as compared with the untreated control (p<0.05) denoted by an *asterisk* (*)

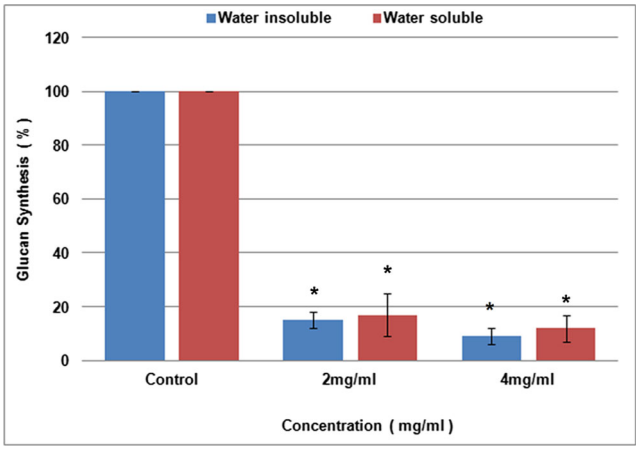

Fig. 5 Inhibitory effect of CaF_2-NPs on the synthesis of water-soluble polysaccharide and water-insoluble polysaccharide (glucans). Data are mean±SD (n=3). Statistical significance as compared with the untreated control (p<0.05) denoted by an *asterisk* (*)

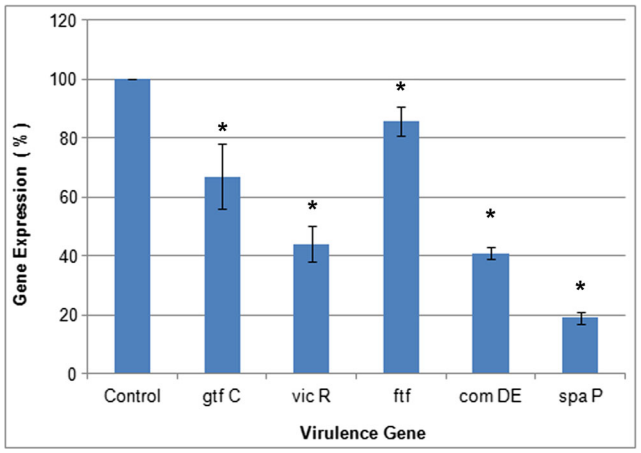

Fig. 7 Expression profile of various genes of *S. mutans* in response to treatment of sub-MIC concentration of CaF_2-NPs. The data presented were generated from at least three independent sets of experiments (data=mean±SD). Statistical significance as compared with the untreated control (p<0.05) denoted by an *asterisk* (*)

indicating that nanoparticles were absolutely nontoxic to the animals used in this study.

In vivo caries reduction

The weekly recovery of *S. mutans* cells over 5 weeks post-treatment is presented in Table S1 of the Supplementary material. There was a substantial decrease in the recovery of *S. mutans* cells from rats treated with nanoparticles as compared to the untreated group (control). It was also found that there was a significant reduction of caries score in rats treated with CaF_2-NPs as compared to the control. Figure 9 shows the reduction in smooth as well as sulcal surface caries after treatment. The overall reduction in smooth surface caries was comparable to sulcal surface caries posttreatment. The severity of smooth surface caries was reduced to 52.6 % (slight), 72.1 % (moderate), and 70.7 % (extensive) as compared to that of sulcal surface caries where they were reduced by 50.8 % (slight), 65.6 % (moderate), and 69.5 % (extensive). However, the reduction in the extensive caries was found to be pronounced over slight and moderate caries.

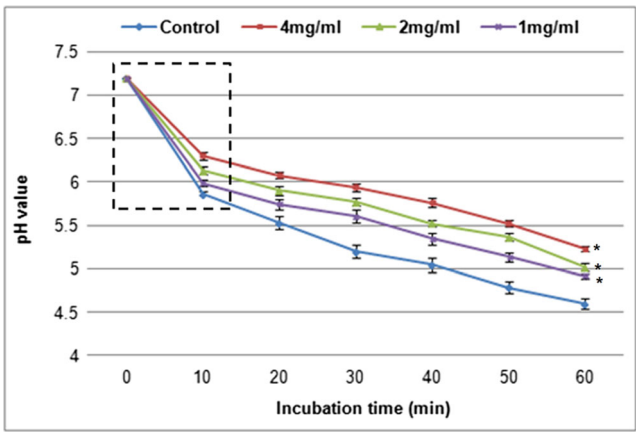

Fig. 6 Effect on sub-MIC levels of CaF_2-NPs on glycolytic pH drop (the values enclosed in a *box* correspond to the initial rate of pH drop). Data are mean±SD (n=3). Statistical significance as compared with the untreated control (p<0.05) denoted by an *asterisk* (*)

Scanning electron micrograph of untreated and treated rats teeth

SEM analysis of the rats' teeth clearly depicted the demineralization of the dental margins in the untreated group (Fig. 10(a)), while the groups treated with CaF_2-NPs showed smooth dental margins as clearly shown in Fig. 10(a′). Furthermore, Fig. 10(b, c, b′, c′) shows the dental surface of untreated and treated teeth, respectively. It was observed that in untreated samples (Fig. 10(b, c)), the surface of the tooth has an evident biofilm embedded in the glucan pool, whereas in the treated groups (Fig. 10(b′, c′)), the dental surface was found clear from any such exopolysaccharide projections as previously detectible in the control.

Discussion

S. mutans is the key organism of dental caries and its cariogenic potentials are well documented (Islam et al. 2008; Dmitriev et al. 2011). The control of its virulence factors like exopolysaccharide production, biofilm formation, aciduracity, and acidogenesis and enhancement of remineralization of tooth enamel are major approaches which can be used for combating dental caries. In the present study, we have reported CaF_2-NPs to be very effective in suppressing *S. mutans* biofilm and other virulence factor (exopolysaccharide formation, acidogenesis, aciduracity).

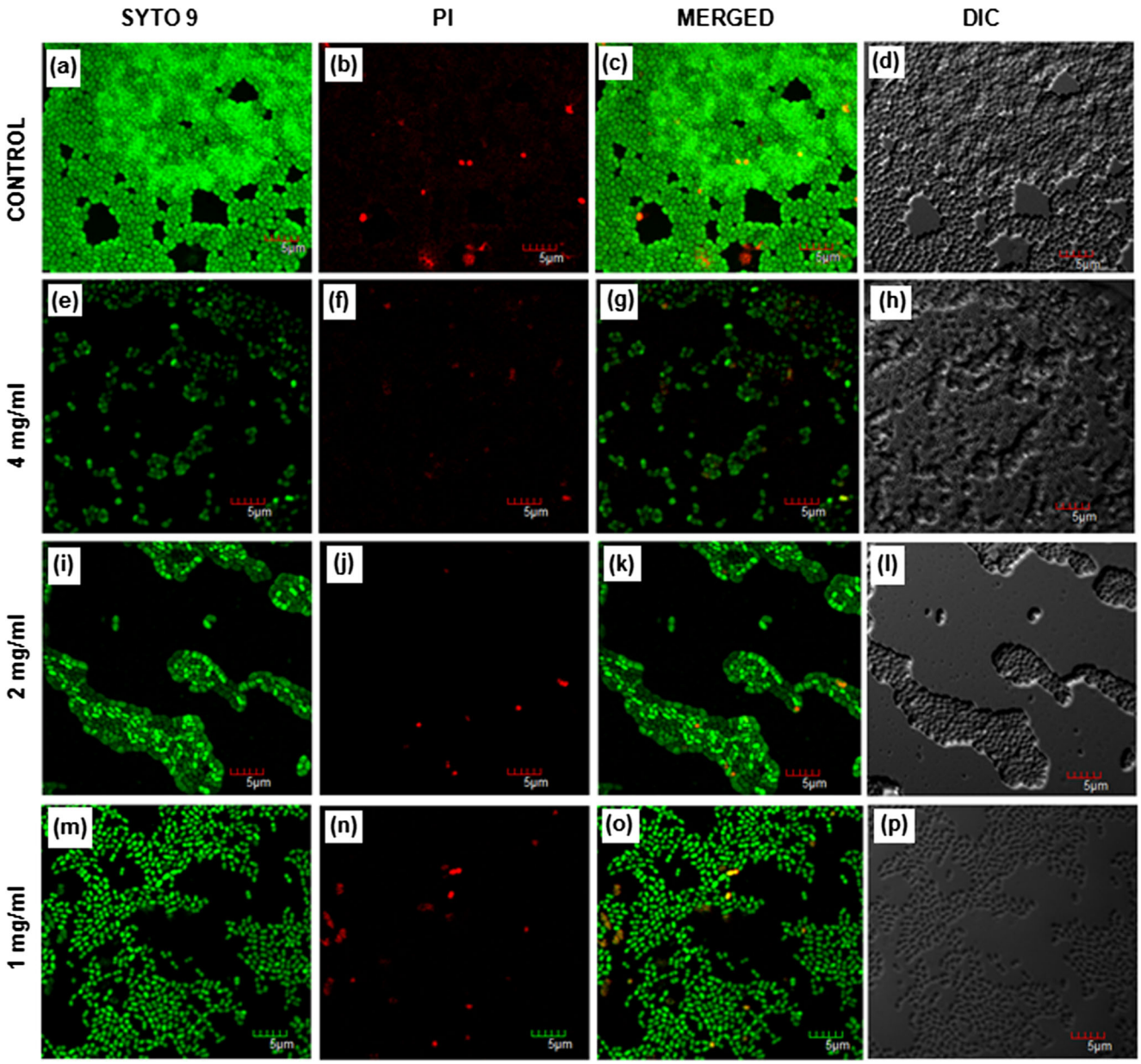

Fig. 8 Effect of CaF_2-NPs on biofilm architecture. Confocal laser scanning micrographs of control biofilm (**a**–**d**) and micrographs of treated biofilm 4 mg/ml (**e**–**h**), 2 mg/ml (**i**–**l**), and 1 mg/ml (**m**–**p**)

CaF_2-NPs were prepared using a co-precipitation method, a type of liquid-phase methods. The main advantages of using liquid-phase methods are simple methodology and high surface activity of the nanomaterials produced (Omolfajr et al. 2011).

Formation of biofilm is the crucial virulence factor of *S. mutans* by virtue of which it causes dental caries (Hamada and Slade 1980; Nance et al. 2013). Biofilms are adherent bacterial communities embedded in the hydrated matrix of exopolysaccharides and exhibit a complex three-dimensional structure (Costerton et al. 1999; Selwitz et al. 2007). The cells in biofilms behave differently in their functionalities as compared to their planktonic counterparts (Fux et al. 2003). Biofilm architecture imparts bacteria with the ability to resist antibiotics and to lead to persistent bacterial infection (Mah and O'Toole 2001). CaF_2-NPs were found to substantially decrease biofilm formation after 24 h of incubation. EPS is essential for the formation, maintenance, and spread of biofilm and it is one of the key virulence factors of *S. mutans* (Flemming and Wingender 2010). A considerable reduction in EPS production in the presence of CaF_2-NPs may be associated with the diminution of the biofilm-forming ability of *S. mutans*. Moreover, the similarity in the growth curve of treated and control samples indicated that CaF_2-NPs reduced biofilm formation without affecting bacterial viability.

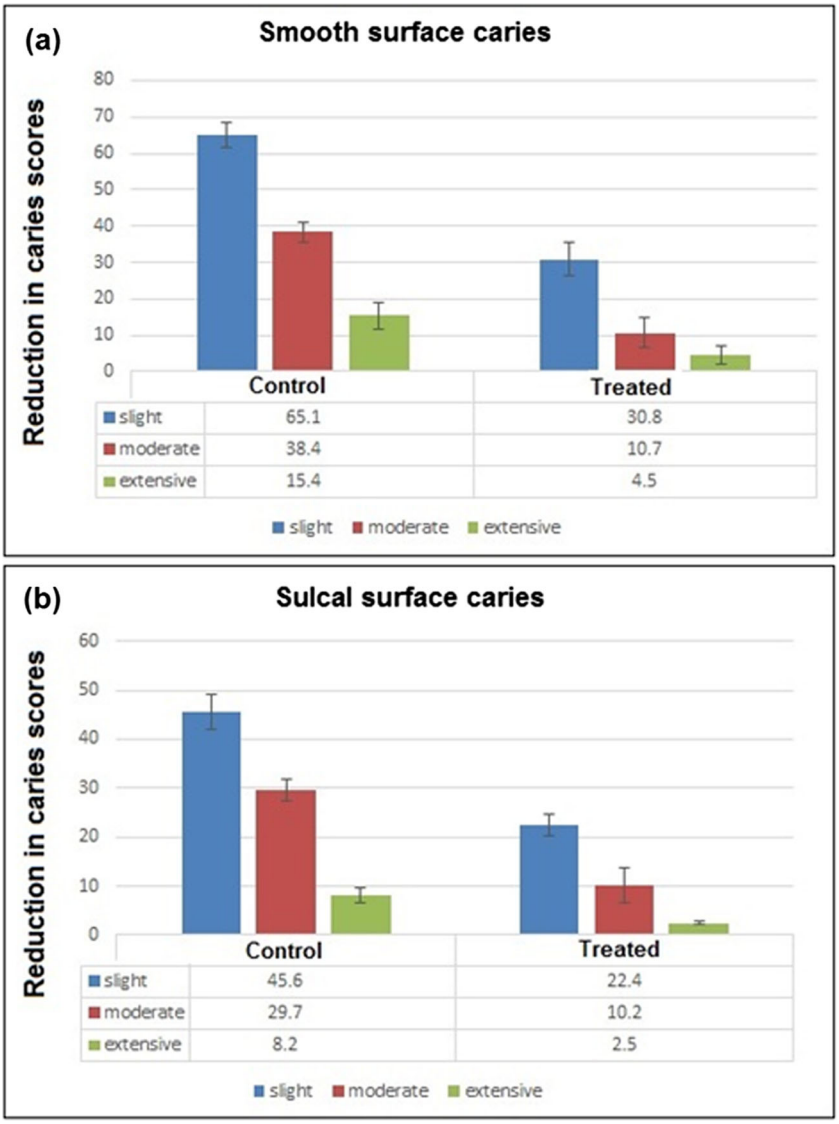

Fig. 9 Effect of sub-MIC level of CaF_2-NPs on dental caries development in rats. **a** Smooth surface caries. **b** Sulcal surface caries; data represents mean±SD of Keyes' score

Attachment of *S. mutans* cells to the adhering surface is a significant step in the process of caries formation, and its deterrence could be a prophylaxis against its virulence (Islam et al. 2008). Adherence occurs mainly by virtue of the hydrophobic interactions between the cells and the adhering surface. The marked inhibition in adherence after short-term exposure of sub-MIC concentrations of CaF_2-NPs showed that the nanoparticles are modifying the physical properties of the cell surface which in turn is reducing the hydrophobic interactions between *S. mutans* and the adhering surface. Moreover, very less reduction in preformed biofilm on treatment with CaF_2-NPs suggests that these nanoparticle are best suited in the prophylactic treatment of dental caries.

Glucan is the main exopolysaccharide produced by *S. mutans* and is an integral component in the sucrose-dependent colonization of *S. mutans* biofilm on the tooth surface. It is elicited from the data that there is a phenomenal reduction in glucan synthesis. Almost equal reduction was observed in both water-soluble and water-insoluble glucans. This indicates that CaF_2-NPs are acting on the GTFs and impairing their enzymatic activity; thus, the reduction in EPS production was due to malfunctioning of GTFs.

Acid production and acid tolerance are cardinal virulence factors which are attributed to the cariogenic ability of *S. mutans* (Kuramitsu 1993). Pursuing these abilities, *S. mutans* easily survives in stress conditions and imposes stress on other species of cariogenic plaque eventually evolving out as the dominant species. Furthermore, the sustained pH values below pH 5.4 aids in the demineralization of the enamel and the development of dental caries (Banas 2004).

The rate of pH drop reflects the acidogenic capacities of the cells, while the final pH values of the suspensions represent acid tolerance (Gregoire et al. 2010). In the present study, the results show a significant drop in the final pH of the suspension in the presence of CaF_2-NPs, suggesting deterioration in

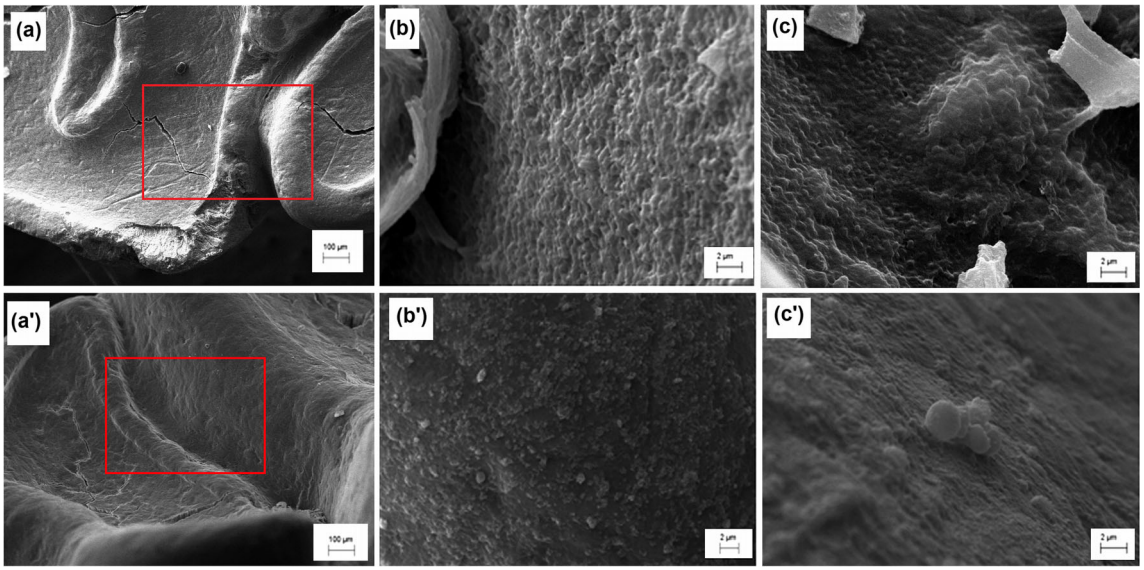

Fig. 10 SEM analysis of rats' teeth to evaluate the effect of CaF_2-NP caries development and extent of demineralization in treated (*lower panel*) and untreated groups (*upper panel*). *a* Untreated rat tooth showing caries (magnification ×200). *b*, *c* Magnified view of marked region showing biofilm of *S. mutans* on untreated tooth (magnification ×10). *a′* CaF_2-NP-treated tooth (magnification ×200). *b′*, *c′* Magnified view of marked region of a treated tooth (magnification ×10)

the acid tolerance capacity of *S. mutans*. Along with this, the rate of pH drop was decreased in the presence of CaF_2-NPs as compared to the control, which implies the impairment of acid production capacity.

It is evident that CaF_2-NPs are acting against some of the major virulence factors of *S. mutans*. One of the reasons behind this antibiofilm property of CaF_2-NPs may be the release of fluoride ions. Fluoride ions have been reported to act directly or, in the form of metal complexes, to inhibit many enzymes (Li 2003). In *S. mutans*, fluoride ions combine with H ions forming the HF molecule, which can eventually inhibit the glycolytic enzymes like enolases (Sutton et al. 1987; Eshed et al. 2013). In addition, a fluoride ion hinders the proton extrusion by F-ATPases through lending a proton back into the cell (Li 2003; Svensäter et al. 2000). Thus, it is possible that suppression of the acid and glucan production ability in the presence of CaF_2-NPs is due to the release of fluoride ions from the nanoparticles.

The gene expression profile of selected genes of *S. mutans* revealed a considerable reduction in gene expression in the presence of CaF_2-NPs. *spaP* (Ag I/II or P1) is a protein of the antigen I/II family and is crucial in *S. mutans* for initial adhesion to the tooth surface (Khan et al. 2010). Downregulation of this gene in *S. mutans* probably results in poor adhesion and reduced ability to form biofilm on smooth surfaces. *vicR* is a two-component regulatory system and is known to regulate a set of genes encoding for important surface proteins which are critical for sucrose-dependent adherence to a smooth tooth surface (Hasan et al. 2012). Thus, suppression of these two genes may further lead to inhibition of adhesion and may be a cause of anticariogenic action. In addition, *gtfC* and *ftf*, which encode the GTFC and FTF enzymes that catalyze the cleavage of sucrose to synthesize extracellular glucan and fructan polysaccharides (He et al. 2012), were also downregulated. The reduction in the aforesaid genes will thereby suppress the exopolysaccharide synthesis pathway eventually inhibiting the biofilm formation. Furthermore, *comDE*, which is a part of the quorum sensing cascade of *S. mutans*, was also suppressed considerably. It has been shown to regulate genetic competence, acid tolerance, and biofilm formation (Li et al. 2002). Hence, downregulation of this gene will not only attenuate internal communication system but also adversely affect the acid tolerance potential of *S. mutans*. As the genes examined are only a selected set of genes of the *S. mutans* genome, additional assessment of other virulence genes is further required to get a broader spectrum of the effect of CaF_2-NPs on cariogenic potentials of *S. mutans*.

The findings of the present study indicated that the antibiofilm effect of CaF_2-NPs against *S. mutans* is a combination of both the suppression in enzymatic activity associated with glucan synthesis and the gene involved in adhesion, acid production, acid tolerance, and quorum sensing. The interaction of CaF_2-NPs with enzymes and the suppression of genes are interlinked to each other at different steps of the regulatory network. This may lead to impairment of the whole metabolic network, eventually forbidding bacterial pathogenesis.

Confocal laser scanning microscopy results were in consistence with the above discussed results. A disruption of biofilm architecture was observed by CLSM in the presence of sub-MIC concentrations of CaF_2-NPs. In the control sample, a green mat is clearly visible which shows that the cells are interacting with each other and forming a healthy biofilm,

while in the treated samples, there were more live cells as compared to dead cells, but less biofilm was formed suggesting that at the tested concentrations there was a tremendous decrease in biofilm formation ability of *S. mutans*. Moreover, TEM images of *S. mutans* are exhibiting insignificant destruction of the peptidoglycan layer, and there was no damage to the cells which validates that CaF_2-NPs is not affecting bacterial viability.

Further, the use of animal models to study the *S. mutans*-host interactions under controlled conditions demonstrated that daily topical exposure to CaF_2-NPs dramatically affected the ability of *S. mutans* to colonize the tooth surfaces, consequently inhibiting the development of smooth surface caries and sulcal surface carious lesions.

These nanoparticles were able to lodge themselves deep into the cavity and could release calcium fluoride in a sustained manner to mineralize the cavity. However, the depth of slight caries was not deep enough to lodge the nanoparticles within them. This is the probable reason for the reduction of extensive caries over the slight and moderate caries. The in vivo effect of CaF_2-NPs was also confirmed by the scanning electron micrographs demonstrating a reduced demineralization and biofilm formation on tooth surfaces treated with CaF_2-NPs. It has been reported that topical application of fluoride on teeth surface results in the formation of calcium fluoride-like material which act as the reservoir of fluoride ions that when released protect the tooth's surface and help in the remineralization (Rosin-Grget and Lincir 2001; Rølla and Saxegaard 1990). Hence, the reduction in caries may be due to the attachment of nanoparticles on the tooth surface and the sustained release of fluoride ions (Sun and Chow 2008; Xu et al. 2008) from CaF_2-NPs, which not only helps in the suppression of virulence traits of *S. mutans* but also promotes remineralization.

Despite the potential benefits of using nanoparticles, it is necessary to be concerned about their probable harmful effects to human health. In the present study, the most likely harmful effect may be the entry of nanoparticles in the human gastrointestinal tract. CaF_2-NPs were found to be noncytotoxic to human normal cell line (HEK-293) and there was no oral toxicity, thus substantiating no detrimental effect on human normal cells. Apart from that, there is a diverse microbial ecosystem in the human intestine and the metabolic activities of these microbes directly actuate human health (Rajilić-Stojanović et al. 2007). Hence, it is important to address the interaction of gut microbes with CaF_2-NPs, and whether these interactions are deleterious, positive, or insignificant. Consequently, further research is required in this aspect before using CaF_2-NPs in therapeutics.

In conclusion, the present study validates the anticariogenic potential of CaF_2-NPs against *S. mutans*. These nanoparticles appear to be ideal for the prevention of dental caries with no oral toxicity. Moreover, they are noncytotoxic to normal human cell line (HEK-293). Thus, CaF_2-NPs could possibly be used as a topical applicant and as a potential therapeutic agent against *S. mutans* to inhibit caries-related problems.

Acknowledgments The authors would like to acknowledge the Advanced Instrumentation Research Facility (J.N.U., India) and Center of Excellence in Material Sciences (A.M.U., India) for providing instrumental support. The authors would also like to acknowledge the Department of Biotechnology (DBT), Government of India, for the support and for allowing the use of the internal facilities of the department. SK thanks BSR-UGC JRF for a fellowship.

Compliance with ethical standards This research was conducted in accordance with institutional ethical standards. The study on animals was approved by the "Interdisciplinary Biotechnology Unit, Institutional Ethical Committee." All applicable international, national, and/or institutional guidelines for the care and use of animals were followed.

Funding This study was supported by a grant from the Council of Scientific and Industrial Research no. 37 (1576) /13/EMR-II.

Conflict of interest All authors declare that they have no competing interests.

References

Banas JA (2004) Virulence properties of *Streptococcus mutans*. Front Biosci 9:1267–1277

Costerton JW, Stewart PS, Greenberg EP (1999) Bacterial biofilms: a cause of persistent infections. Science 284:1318–1322

Denizot F, Lang R (1986) Rapid colorimetric assay for cell growth and survival. Modifications to the tetrazolium dye procedure giving improved sensitivity and reliability. J Immunol Meth 89:271–277

Dmitriev A, Mohapatra SS, Chong P, Neely M, Biswas S, Biswas I (2011) CovR controlled global regulation of gene expression in *Streptococcus mutans*. PLoS One 6:e2012

Dubois M, Gilles KA, Hamilton JK, Rebers PA, Smith F (1956) Colorimetric method for determination of sugars and related substances. Anal Chem 28:350–356

Eshed M, Lellouche J, Banin E, Gedanken A (2013) MgF_2 nanoparticle-coated teeth inhibit *Streptococcus mutans* biofilm formation on a tooth model. J Mater Chem B 1:3985

Falsetta ML, Klein MI, Colonne PM, Scott-Anne K, Gregoire S, Pai CH, Gonzalez M, Watson G, Krysan DJ, Bowen WH, Koo H (2014) Symbiotic relationship between *Streptococcus mutans* and *Candida albicans* synergizes the virulence of plaque-biofilms in vivo. Infect Immun 82:1968–1981

Featherstone JDB (1999) Prevention and reversal of dental caries: role of low level fluoride. Community Dent Oral Epidemiol 27:31–40

Flemming HC, Wingender J (2010) The biofilm matrix. Nat Rev Microbiol 8:623–633

Fujihara S, Kadota Y, Kimura T (2002) Role of organic additives in the sol-gel synthesis of porous CaF_2 anti-reflective coatings. J Sol-Gel Sci Technol 24:147–154

Fux CA, Stoodley P, Hall-stoodley L, Costerton JW (2003) Bacterial biofilms: a diagnostic and therapeutic challenge. Expert Rev Anti Infect Ther 1(4):667–683

Gregoire S, Singh AP, Vorsa N, Koo H (2010) Influence of cranberry phenolics on glucan synthesis by glucosyltransferases and *Streptococcus mutans* acidogenicity. J Appl Microbiol 103:1960–1968

Hamada S, Slade HD (1980) Biology, immunology, and cariogenicity of *Streptococcus mutans*. Microbiol Rev 44(2):331–384

Hamilton IR (1977) Effects of fluoride on enzymatic regulation of bacterial carbohydrate metabolism. Caries Res 11:262–291

Hasan S, Danishuddin M, Adil M, Singh K, Verma PK, Khan AU (2012) Efficacy of *E. officinalis* on the cariogenic properties of *Streptococcus mutans*: a novel and alternative approach to suppress quorum-sensing mechanism. Plos One 7:e40319

Hasan S, Danishuddin M, Khan AU (2015) Inhibitory effect of *Zingiber officinale* towards *Streptococcus mutans* virulence and caries development: in vitro and in vivo studies. BMC Microbiol 15(1):1

He Z, Wang Q, Hu Y, Liang J, Jiang Y, Ma R, Tang Z, Huang Z (2012) Use of the quorum sensing inhibitor furanone C-30 to interfere with biofilm formation by *Streptococcus mutans* and its *luxs* mutant strain. Int J Antimicrob Agents 40:30–35

Hernández-Sierra JF, Ruiz F, Cruz Pena DCC, Martínez-Gutiérrez F, Martínez AE, de Jesús Pozos Guillén AJP, Tapia-Pérez H, Martínez Castañón GM (2008) The antimicrobial sensitivity of *Streptococcus mutans* to nanoparticles of silver, zinc oxide, and gold. Nanomedicine 4:237–240

Islam B, Khan SN, Haque I, Alam M, Mushfiq M, Khan AU (2008) Novel anti-adherence activity of mulberry leaves: inhibition of *Streptococcus mutans* biofilm by 1-deoxynojirimycin isolated from *Morus alba*. J Antimicrob Chemother 62:751–757

Khan R, Zakir M, Khanam Z, Shakil S, Khan AU (2010) Novel compound from *Trachyspermum ammi* (*Ajowan caraway*) seeds with antibiofilm and anti adherence activities against *Streptococcus mutans*: a potential chemotherapeutic agent against dental caries. J Appl Microbiol 109:2151–2159

Khan S, Alam F, Azam A, Khan AU (2012) Gold nanoparticle enhanced methylene blue-induced photodynamic therapy: a novel therapeutic approach to inhibit *Candida albicans* biofilm. Int J Nanomedicine 7: 3245–3257

Khan ME, Alam F, Parveen A, Naqvi AH (2013) structural, optical and dielectric properties of alkaline earth metal (Sr 0.05, Mg 0.05 and Ba 0.05) doped CaF_2 nanoparticles and their microscopic analysis. J Adv Microsc Res 8:45–52

Koo H, Hayacibara MF, Schobel BD, Cury JA, Rosalen PL, Park YK, Vacca-smith AM, Bowen WH (2003) Inhibition of *Streptococcus mutans* biofilm accumulation and polysaccharide production by apigenin and tt-farnesol. J Antimicrob Chemother 52:782–789

Krol JE, Biswas S, King C, Biswas I (2014) SMU.746-SMU.747, a putative membrane permease complex, is involved in aciduricity, acidogenesis, and biofilm formation in *Streptococcus mutans*. J Bacteriol 196:129–139

Kulshrestha S, Khan S, Meena R, Singh BR, Khan AU (2014) A graphene/zinc oxide nanocomposite film protects dental implant surfaces against cariogenic *Streptococcus mutans*. Biofouling 30(10):1281–1294

Kumar GA, Chen CW, Ballato J, Riman RE (2007) Optical characterization of infrared emitting rare-earth-doped fluoride nanocrystals and their transparent nanocomposites. Chem Mater 19:1523–1528

Kuramitsu HK (1993) Virulence factors of *mutans Streptococci*: role of molecular genetics. Crit Rev Oral Biol Med 4:159–176

Larson RM (1981) Merits and modifications of scoring rat dental caries by Keyes' method. In: Tanzer JM (ed) Animal models in cariology. Microbiology abstracts (special suppl.). IRL, Washington, pp 195–203

Li L (2003) The biochemistry and physiology of metallic fluoride: action, mechanism, and implications. Crit Rev Oral Biol Med 14:100–114

Li Y-H, Tang N, Aspiras MB, Lau PC, Lee JH, Ellen RP, Cvitkovitch DG (2002) A quorum-sensing signalling system essential for genetic competence in *Streptococcus mutans* is involved in biofilm formation. J Bacteriol 184(10):2699–2708

Livak KJ, Schmittgen TD (2001) Analysis of relative gene expression data using real-time quantitative PCR and the $2^{-\Delta\Delta CT}$ method. Methods 25(4):402–408

Loesche WJ (1986) Role of *Streptococcus mutans* in human dental decay. Microbiol Rev 50:353–380

López-Moreno A, Sepúlveda-Sánchez JD, Mercedes Alonso Guzmán MMA, Le Borgne SL (2014) Calcium carbonate precipitation by heterotrophic bacteria isolated from biofilms formed on deteriorated ignimbrite stones: influence of calcium on EPS production and biofilm formation by these isolates. Biofouling 30:547–560

Mah TC, O'Toole GA (2001) Mechanisms of biofilm resistance to antimicrobial agents. Trends Microbiol 9:34–39

Marquis RE, Clock SA, Mota-Meira M (2003) Fluoride and organic weak acids as modulators of microbial physiology. FEMS Microbiol Rev 26:493–510

Nakano K, Nomura R, Nemoto H, Mukai T, Yoshioka H, Shudo Y, Hata H, Toda K, Taniguchi K, Amano A, Ooshima T (2007) Detection of novel serotype k *Streptococcus mutans* in infective endocarditis patients. J Med Microbiol 56:1413–1415

Nance WC, Dowd SE, Samarian D, Chludzinski J, Delli J, Battista J, Rickard AH (2013) A high-throughput microfluidic dental plaque biofilm system to visualize and quantify the effect of antimicrobials. J Antimicrob Chemother 68:2550–2560

Omolfajr N, Nasser S, Mahmood R, Kompany A (2011) Synthesis and characterization of CaF_2 NPs with co-precipitation and hydrothermal methods. J Nanomed Nanotechnol 2:5

Pandurangappa C, Lakshminarasappa BN (2011a) Optical absorption and photoluminescence studies in gamma-irradiated nanocrystalline CaF_2. Nanosci Nanotechnol 2:108

Pandurangappa C, Lakshminarasappa BN (2011b) Optical studies of samarium-doped fluoride nanoparticles. Philos Mag 91:35

Phan TN, Buckner T, Sheng J, Baldeck JD, Marquis RE (2004) Physiologic actions of zinc related to inhibition of acid and alkali production by oral *Streptococci* in suspensions and biofilms. Oral Microbiol Immunol 19:31–38

Raghupathi KR, Koodali RT, Manna AC (2011) Size-dependent bacterial growth inhibition and mechanism of antibacterial activity of zinc oxide nanoparticles. Langmuir 27:4020–4028

Rajilić-Stojanović M, Smidt H, de Vos WM (2007) Diversity of the human gastrointestinal tract microbiota revisited. Environ Microbiol 9: 2125–2136

Rølla G, Saxegaard E (1990) Critical evaluation of the composition and use of topical fluorides with emphasis on the role of calcium fluoride in caries inhibition. J Dent Res 69(2 Suppl):780–785

Rosin-Grget K, Lincir I (2001) Current concept on the anticaries fluoride mechanism of the action. Coll Antropol 25(2):703–712

Saxegaard E, Rølla G (1989) Kinetics of acquisition and loss of calcium fluoride by enamel in vivo. Caries Res 23:406–411

Selwitz RH, Ismail AI, Pitts NB (2007) Dental caries. Lancet 369:51–59

Sun L, Chow LC (2008) Preparation and properties of nano-sized calcium fluoride for dental applications. Dent Mater 24(1):111–116

Sutton SV, Bender GR, Marquis RE (1987) Fluoride inhibition of proton-translocating ATPases of oral bacteria. Infect Immun 55(11):2597–2603

Svensäter G, Sjögreen B, Hamilton IR (2000) Multiple stress responses in *Streptococcus mutans* and the induction of general and stress-specific proteins. Microbiology 146:107–117

Xu HHK, Moreau J, Sun L, Chow LC (2008) Strength and fluoride release characteristics of a calcium fluoride based dental nanocomposite. Biomaterials 29(32):4261–4267

Zhang X, Quan Z, Yang J, Yang P, Lian H, Lin J (2008) Solvothermal synthesis of well dispersed MF_2 (M = Ca, Sr, Ba) nanocrystals and their optical properties. Nanotechnology 19:075603